

Photomechanical Bending and Photosalient Effect of Flexible Crystals of an Acylhydrazone

Pragyan J. Hazarika,^a Poonam Gupta,^a Suryanarayana Allu,^b and Naba K Nath^{a*}

^a Department of Chemistry, National Institute of Technology, Meghalaya 793003, India

^b Department of Chemical Engineering (Integrated Engineering), Kyung Hee University,

Yongin 17104, South Korea.

Content of Supporting Information

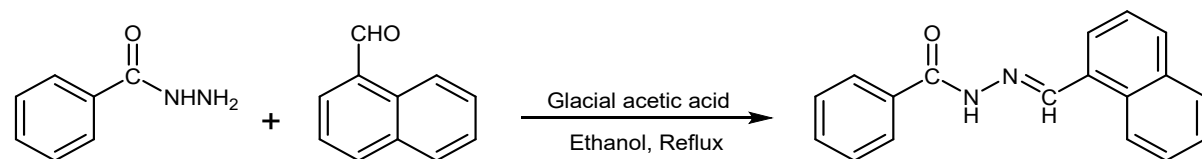
1. Supporting Methods	
1.1 Materials	S3
1.2 Synthesis and characterization of acylhydrazone derivative (Ach)	S3
1.3 Instrumentation	S3-S4
1.4 Computational Studies	S4
2. Supporting figures	
Figure S1. Thermal microscopy images Ach crystal	S5
Figure S2. FT-IR spectra of Ach	S5
Figure S3. ¹ H-NMR of Ach in DMSO-d ₆ solvent	S6
Figure S4. ORTEP of Ach	S6
Figure S5. Face indexing of the crystal of Ach	S7
Figure S6. Radius of curvature of the bent crystals of Ach	S7
Figure S7. Solution state photoswitching of Ach in acetonitrile solution	S8
Figure S8. Solid-state photoswitching of Ach recorded on a KBr pellet	S8
Figure S9. DFT-optimized geometry, frontier molecular orbitals and HOMO–LUMO energy gaps of Ach	S9
Figure S10. Computed UV-vis spectra of Ach	S9
Figure S11. ¹ H NMR spectra recorded on a photo irradiated crystalline sample of Ach	S10
Figure S12. Heat-induced straightening of a bent crystal	S10
Figure S13. Photomechanical effect of Ach crystals in different UV light power density	S11-S25
3. Supporting tables.	
Table S1. Basic crystallographic parameters of Ach	S26
Table S2. Summary of TD-DFT calculations for Ach (<i>E</i>) and Ach (<i>Z</i>)	S27
Table S3. Mathematical equations used to calculate the various quantifiable parameters	S27
Table S4. Dimensions of 75 crystals of Ach and their corresponding time to display PS	S28-S30
4. Optimized coordinates of Ach in its two forms	S30-S32
5. Supporting references	S33
6. Supporting videos	S33

1. Supporting Methods

1.1

Materials: Without any further purification, the following materials were used from their respective commercial sources: Benzhydrazide (from Alfa Aesar), 1-naphthaldehyde (from Alfa Aesar), ethanol (from CSS), glacial acetic acid (from Himedia), acetonitrile (from Spectrochem).

1.2 Synthesis and characterization of acylhydrazone derivative (**Ach**):



Scheme S1. Synthetic scheme of **Ach**.

Ach was synthesised by following a previously mentioned procedure.^{S1} In this reaction, 1-naphthaldehyde (1.0 equivalent) was added into a round bottom flask containing the equimolar amount of Benzhydrazide (1.0 equivalent) dissolved in ethanol, and the whole reaction mixture was refluxed for 4–5 hrs after the addition of a few drops of glacial acetic acid as a catalyst. After the completion of the reaction, the obtained white precipitate was separated by filtering in a Buchner funnel, and the product was recrystallized from acetonitrile. The compound, **Ach** was then characterized by melting point determination (Figure S1), FT-IR spectroscopy (Figure S2), ¹H NMR (Figure S3) and single-crystal X-ray diffraction (Figure S4 and Table S1).

Ach: Yield: 81%. Melting point: ~164 °C.

FT-IR:

3227 cm⁻¹, 1644 cm⁻¹, 1542 cm⁻¹.

¹H NMR 500

MHz, DMSO-d6) δ 11.92 (s, 1H), 9.12 (s, 1H), 8.87 (d, J = 8.4 Hz, 1H), 8.08 – 8.00 (m, 2H), 7.96 (dd, J = 16.1, 7.2 Hz, 3H), 7.68 (d, J = 7.8 Hz, 1H), 7.65 – 7.59 (m, 3H), 7.57 (t, J = 7.3 Hz, 2H).

1.3 Instrumentation:

Thermal

microscopy: The samples were put on a thermal stage (Linkam) fitted with a microscope (Leica DM 2700P) and a camera (Leica MC170HD) to measure the melting point of the synthesized compounds.

FT-IR spectroscopy: FT-IR spectra were recorded in UATR mode using the Perkin Elmer FT-IR spectrometer.

¹H NMR Spectroscopy: The NMR spectra were collected using Bruker Avance spectrometer (500 MHz and 400 MHz) and at 25 °C. Chemical shifts (in ppm) are given relative to the non-deuterated residual solvent signals of DMSO-D6 (δ = 2.5 ppm).

Single crystal X-ray diffraction: Single crystal X-ray diffraction patterns were obtained by employing Bruker D8 QUEST Eco CCD single crystal X-ray diffractometer with MoK α source ($\lambda = 0.71073 \text{ \AA}$) and a fine-focus sealed tube. The Apex II program^{S2} was used to capture the diffraction frames and then they were integrated using Bruker SAINT.^{S3} SADABS was used to carry out the absorption correction.^{S4} The crystal structure was analyzed and refined using the SHELX^{S5-S7} program and OLEX2^{S8}.

UV-Visible spectroscopy: The UV-vis spectra were acquired using the Perkin Elmer UV-vis spectrometer (in solution state Lambda 35 and in solid state Lambda 365). UV light, obtained from a mercury-xenon lamp with a wavelength of 365 nm and a power density of 361 mW cm $^{-2}$ was irradiated on the solutions to investigate the photoswitching behavior of the synthesized compound.

Mechanical effects: Photomechanical bending motion and reversible physical deformation of the synthesised crystals were studied under Leica M80 microscope. The videos and pictures were recorded by using MC170HD camera mounted in the microscope and were analysed with the LAS software (ver. 4.9.0). Mercury-xenon UV lamp (Hamamatsu Photonics, LC8 UV spotlight source, model L9566-01A) fixed to a heat filter (Hamamatsu Photonics, model A9616-05, wavelength range 300–450 nm) was used to study the photoresponsive nature of the crystals. The UV power density was recorded by using a precalibrated light power meter (Hamamatsu, model C6080-365-03).

1.4 Computational Studies:

DFT

and TD-DFT studies: Geometry optimization for the compound **Ach** was carried out using Density Functional Theory (DFT) in Gaussian 09 software package^{S9} with Becke3-Lee-Yang-Parr (B3LYP) functional^{S10} and 6-31G(d)^{S11,S12} basis set. Further, those optimized geometries were used to perform Time-Dependent Density Functional Theory (TD-DFT) with the same functional and basis set to obtain the theoretical UV spectra.

2. Supporting Figures

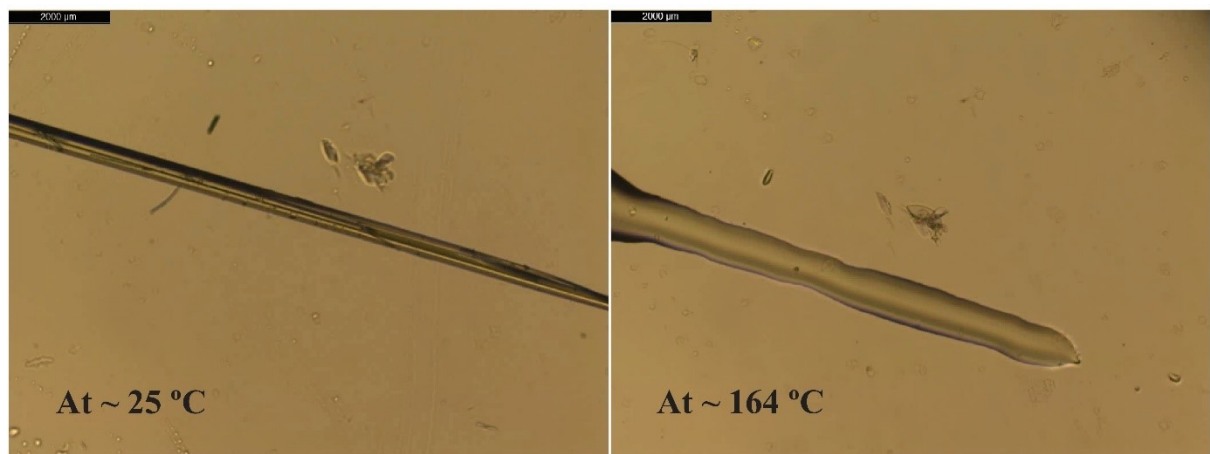


Figure S1. Thermal microscopy images show the melting of Ach crystal.

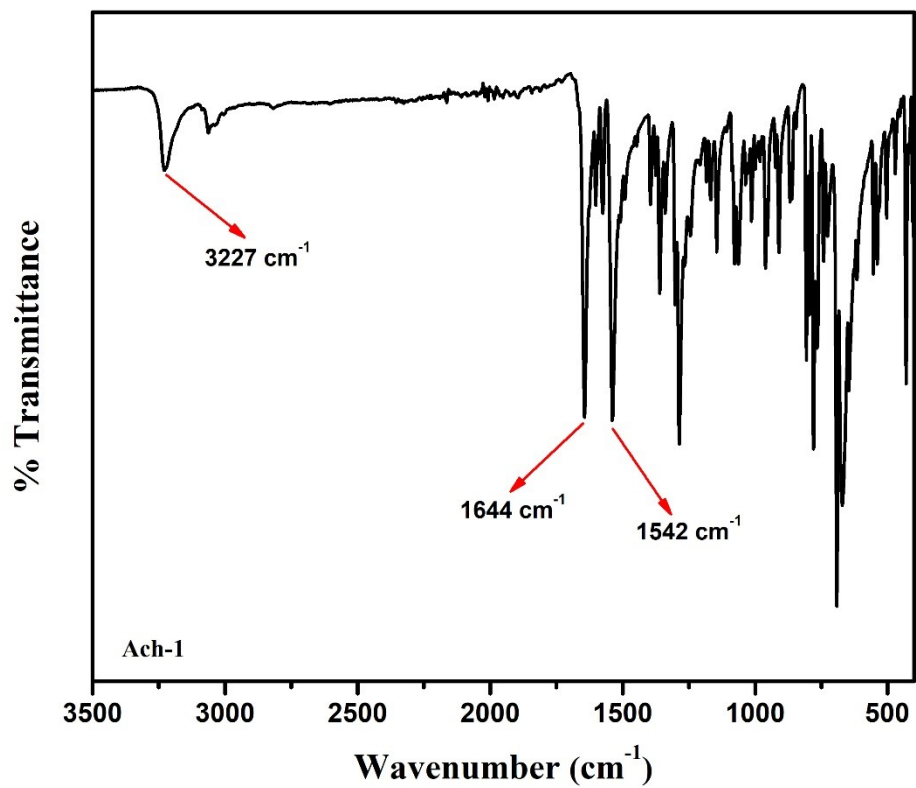


Figure S2. FT-IR spectra of Ach.

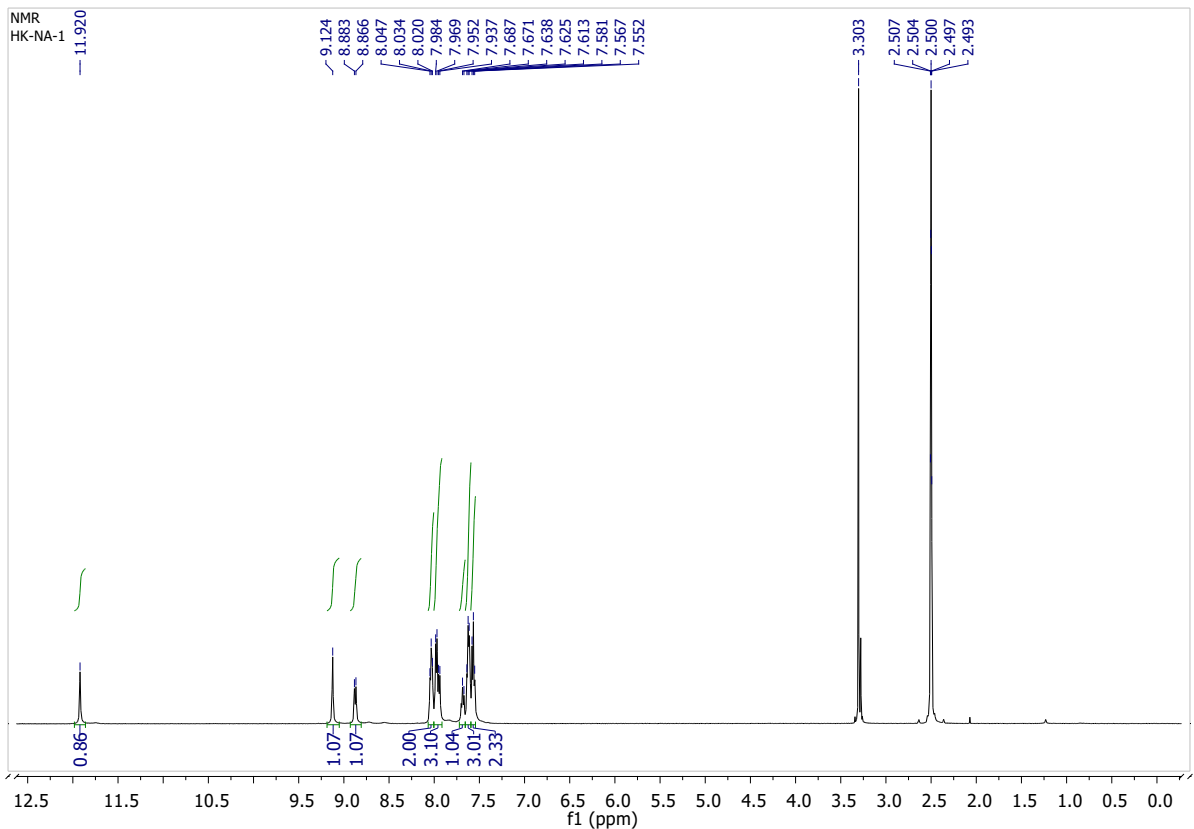


Figure S3. ^1H -NMR of Ach in DMSO-d₆ solvent.

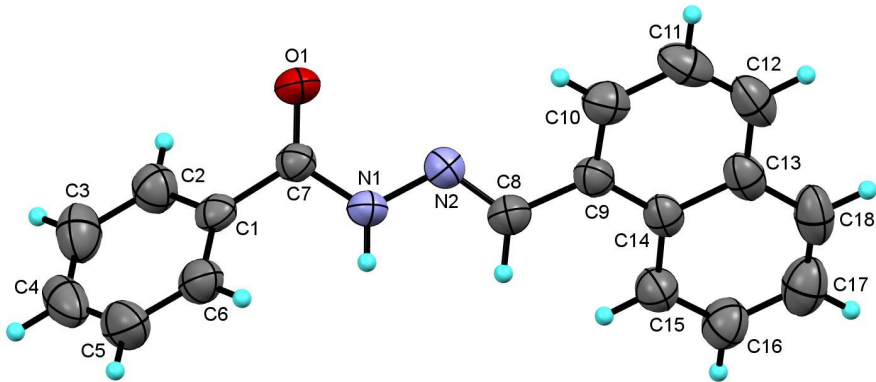


Figure S4. ORTEP diagram of Ach with 50% probability ellipsoid.

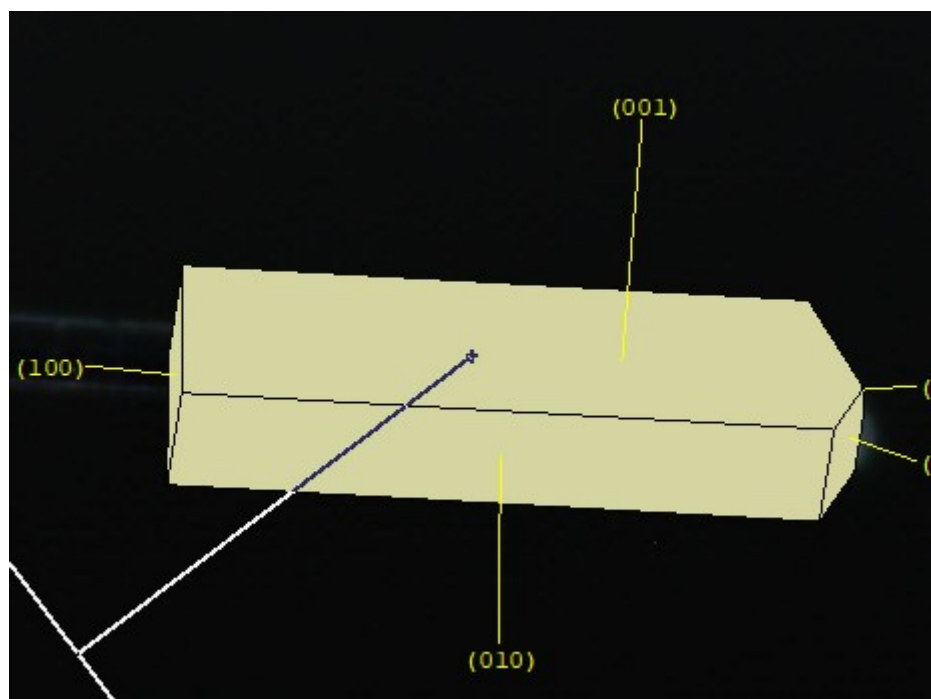


Figure S5. Face indexing of the crystal of Ach.

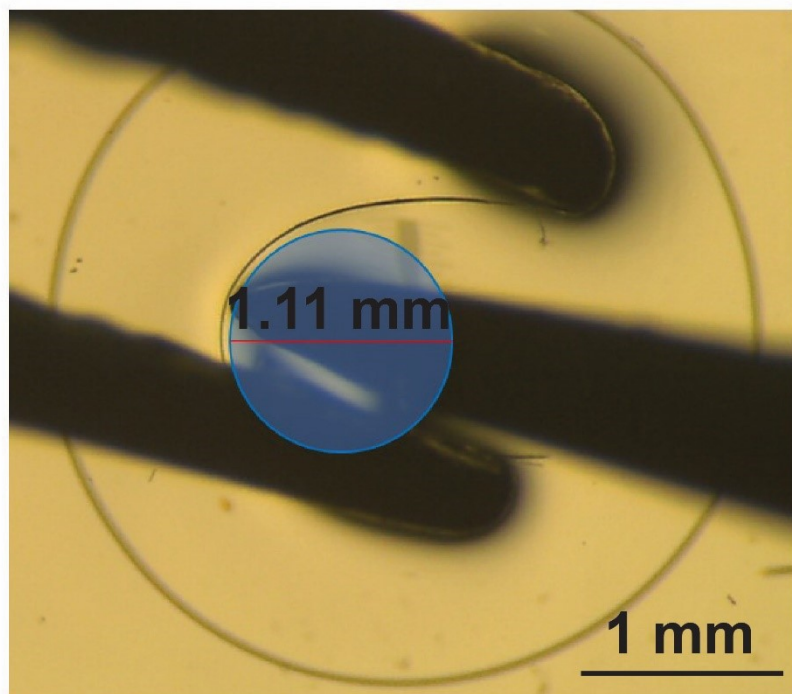


Figure S6. The radius of curvature of the bent crystals of Ach.

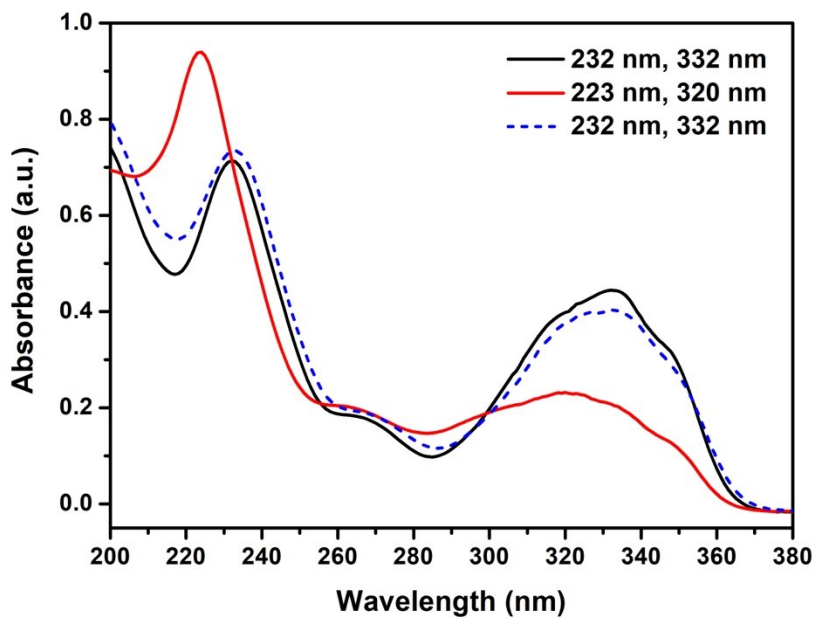


Figure S7. Solution state photoswitching of **Ach** in acetonitrile solution. The *Z* to *E* conversion is achieved by heating. The black line indicates spectra before UV irradiation, the red line indicates spectra after 5 seconds of UV irradiation, and the blue dotted line indicates spectra after heating the solution at 50 °C for 50 minutes.

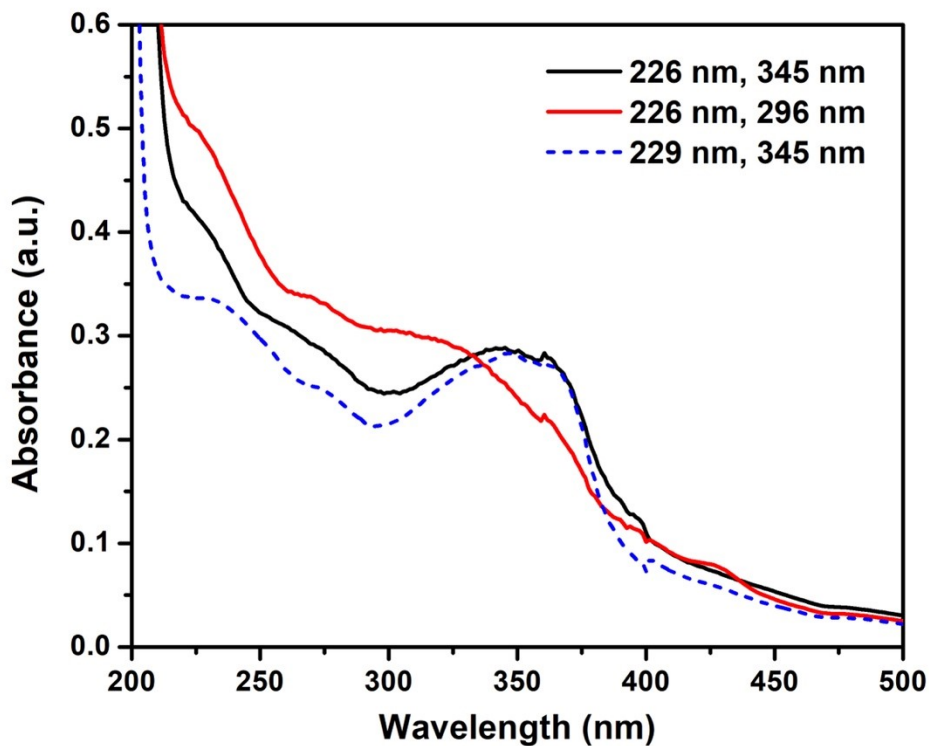


Figure S8. Solid-state UV visible spectra were recorded on a KBr pellet of **Ach**. The black line represents spectra before UV irradiation, the red line represents spectra after UV irradiation, and the blue dotted line represents spectra after heating the sample with a warm LED light.

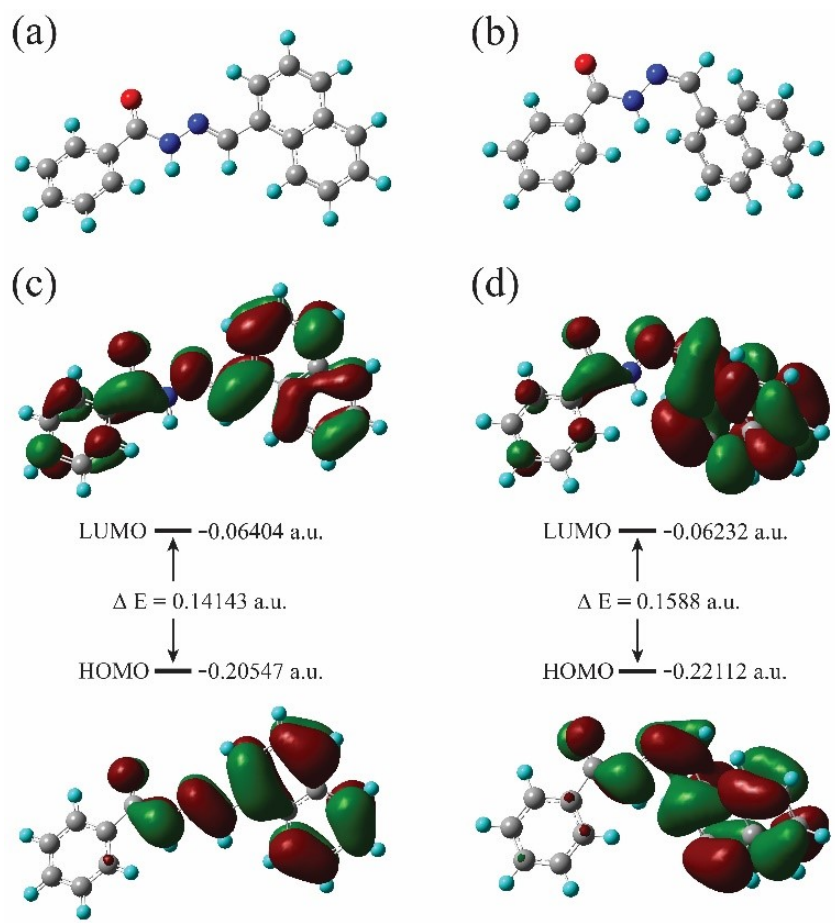


Figure S9. DFT-optimized geometry, frontier molecular orbitals and HOMO–LUMO energy gaps of Ach in its two different isomeric forms (a,c) *E* and (b,d) *Z*.

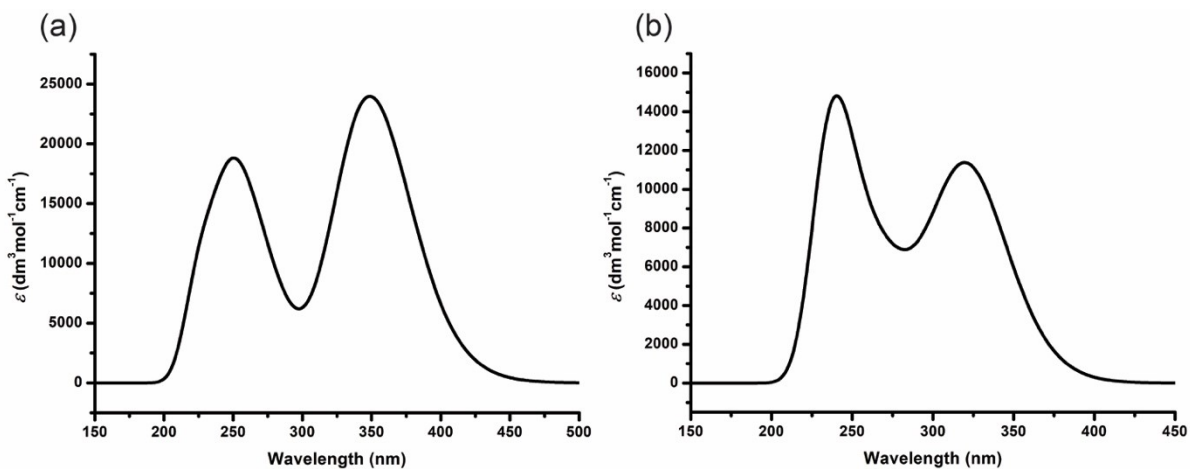


Figure S10. UV–vis absorption spectrum of (a) Ach (*E*), (b) Ach (*Z*) obtained from TD-DFT calculations at B3LYP/6-31G(d) level.

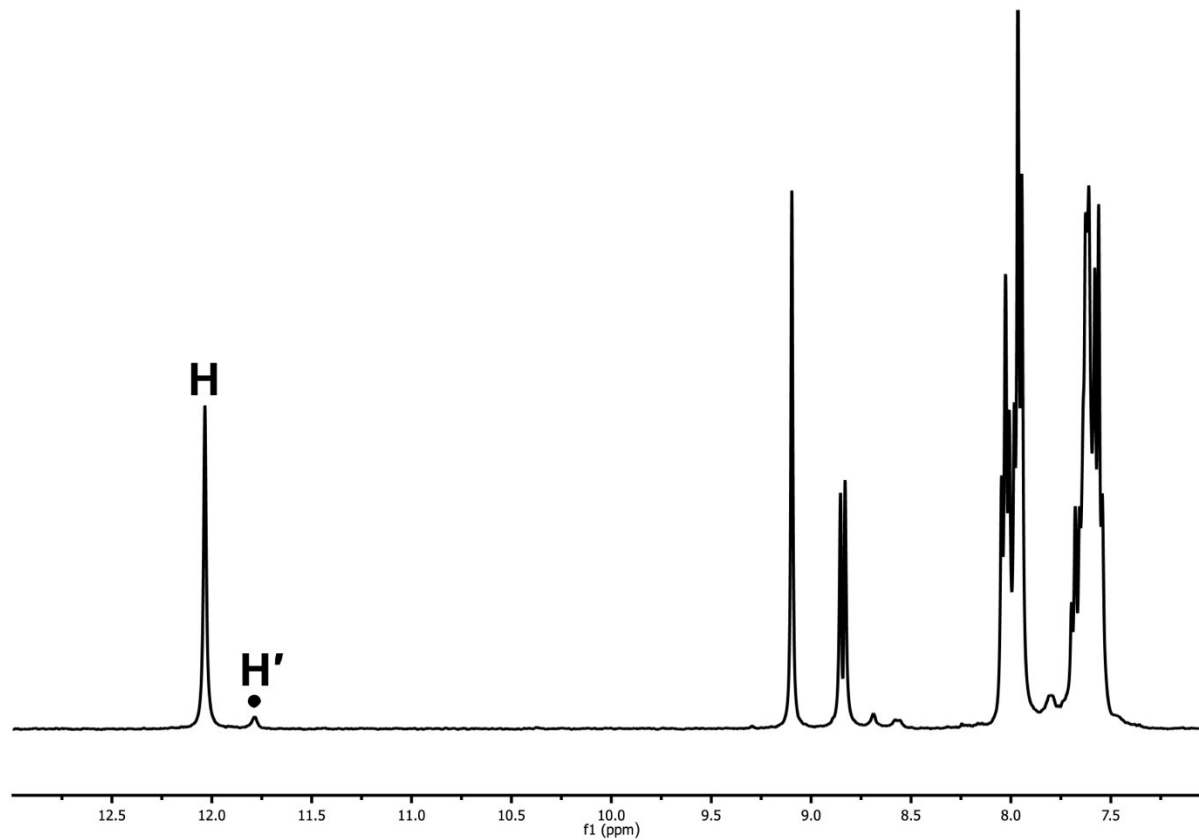


Figure S11. ^1H NMR spectra recorded on a photo irradiated crystalline sample of **Ach** in DMSO-D₆ solvent indicated the presence of both *E* and *Z* isomer. The H and H' represent N—H protons of *E* and *Z* isomers, respectively.

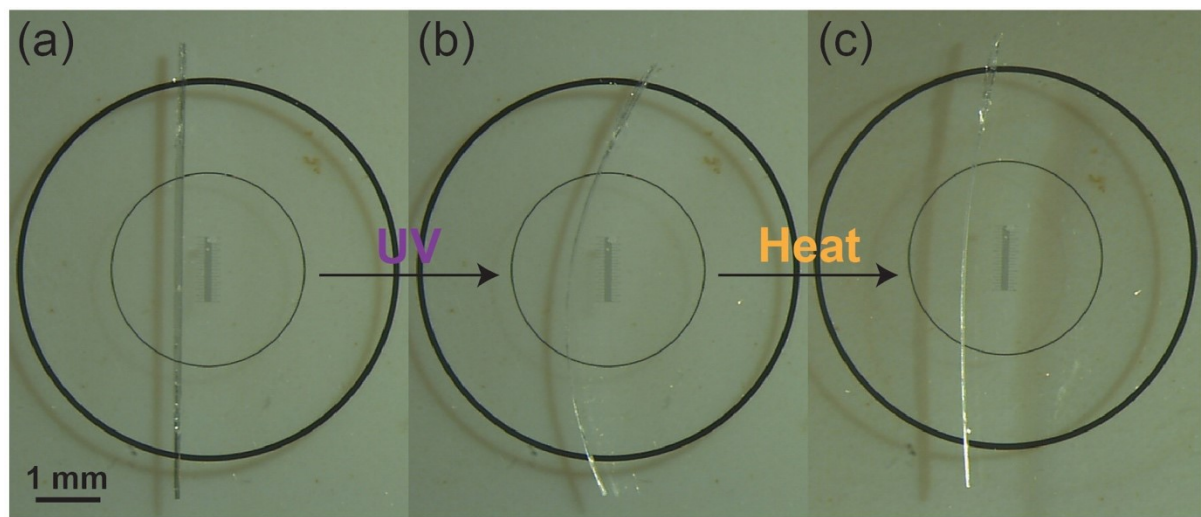
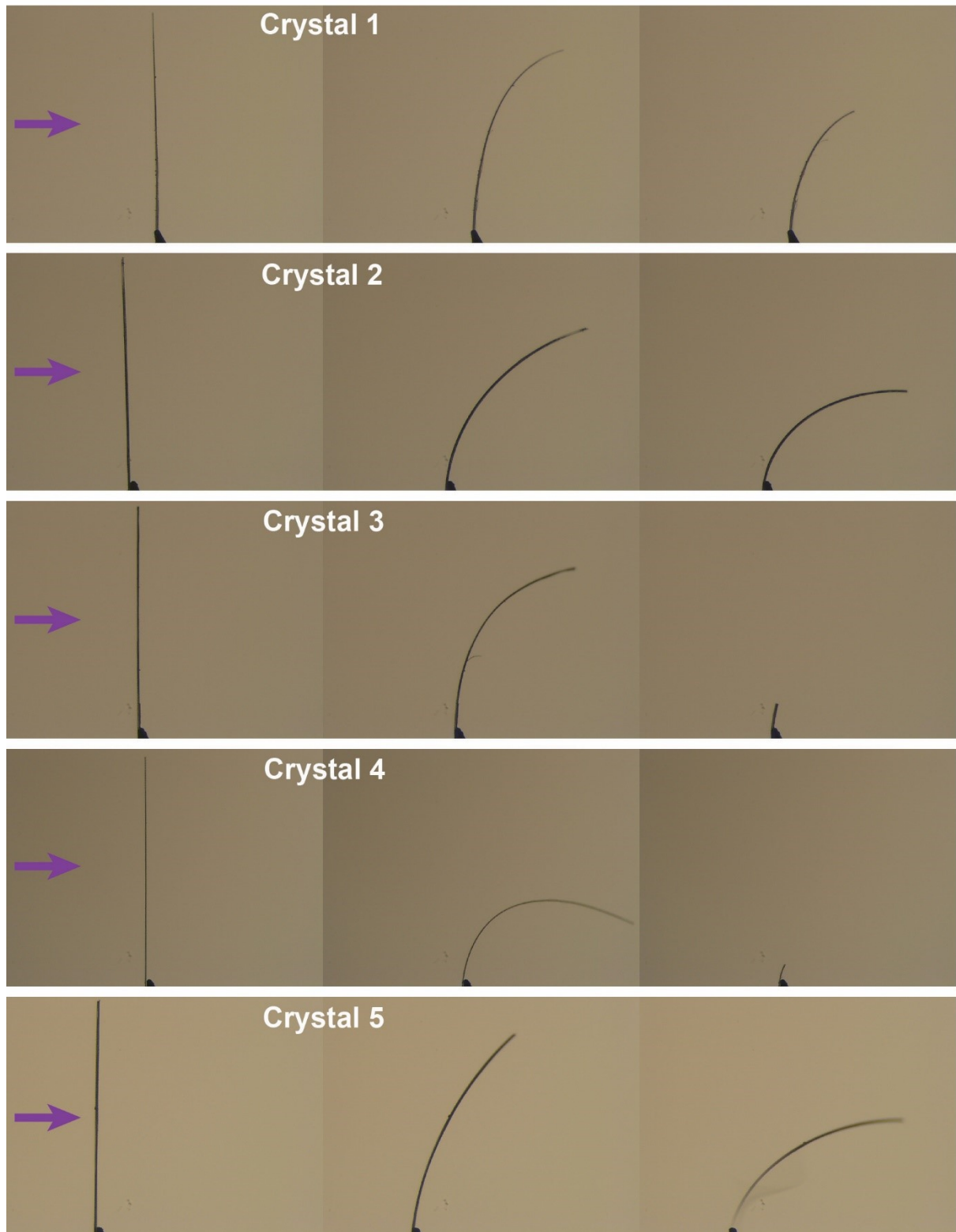
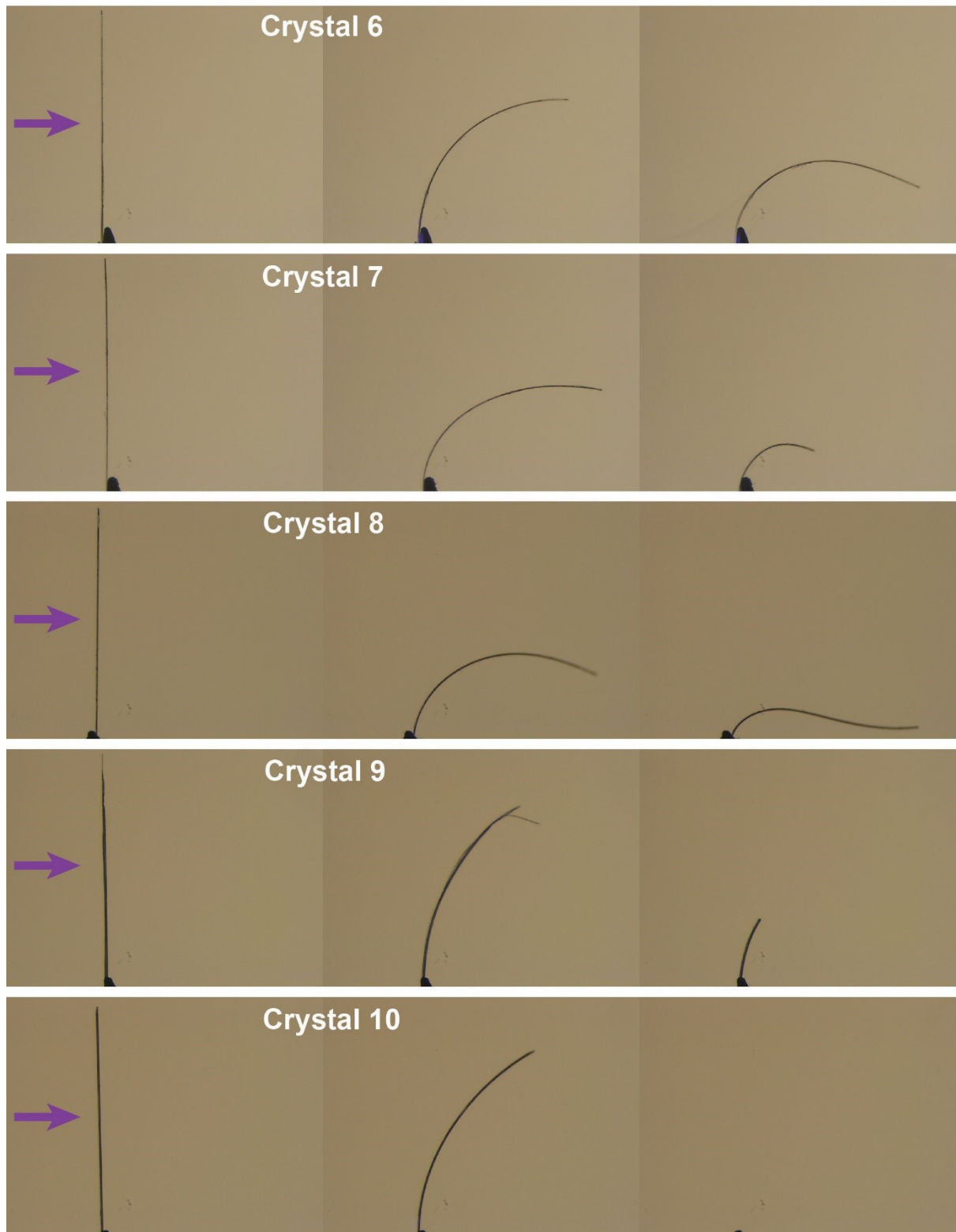


Figure S12. (a) Straight crystal of **Ach**, (b) bent by shining UV light. (c) When heated to 65 °C for one hour almost regained its original straight shape.

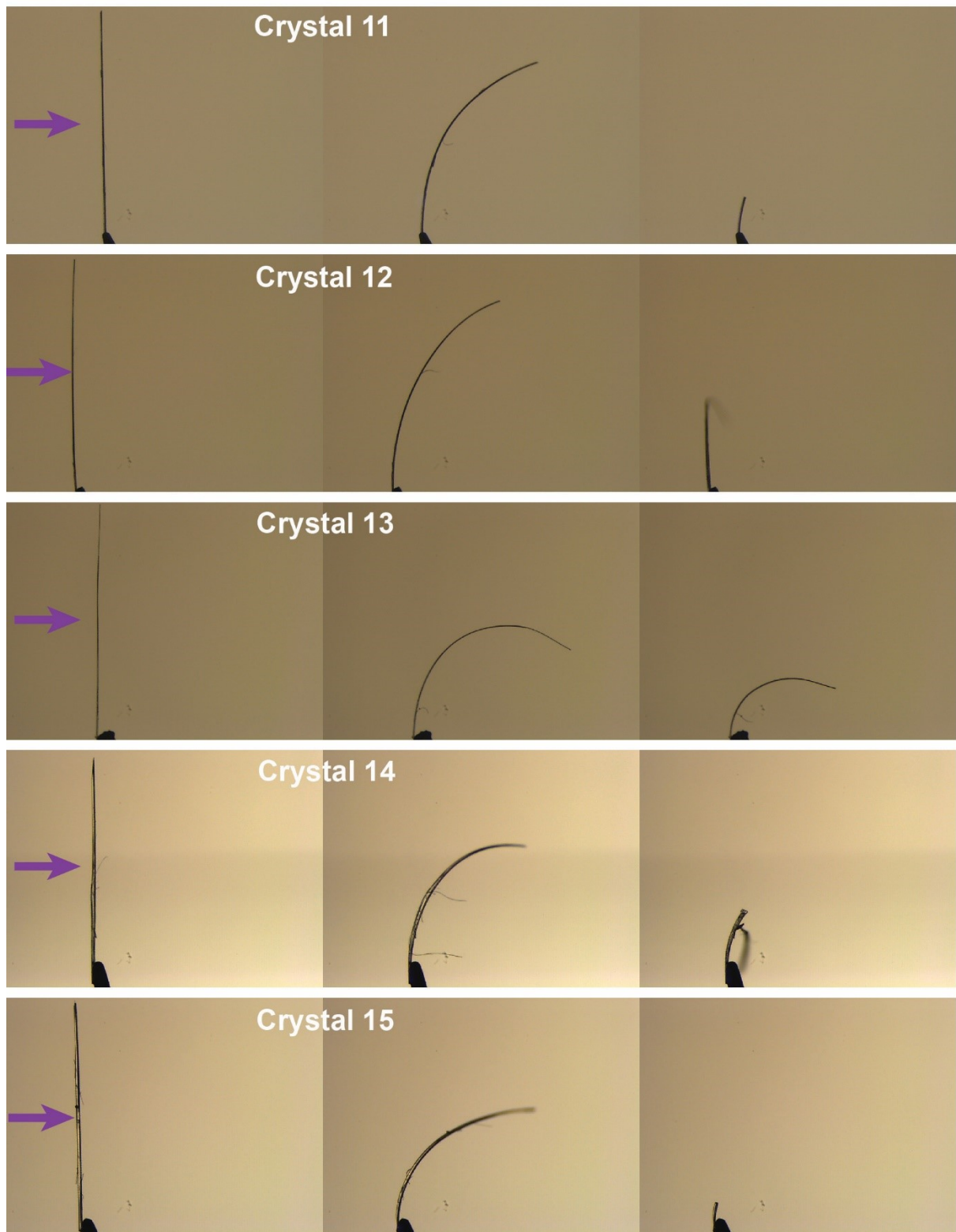
UV light power density (29.1 mW cm^{-2})



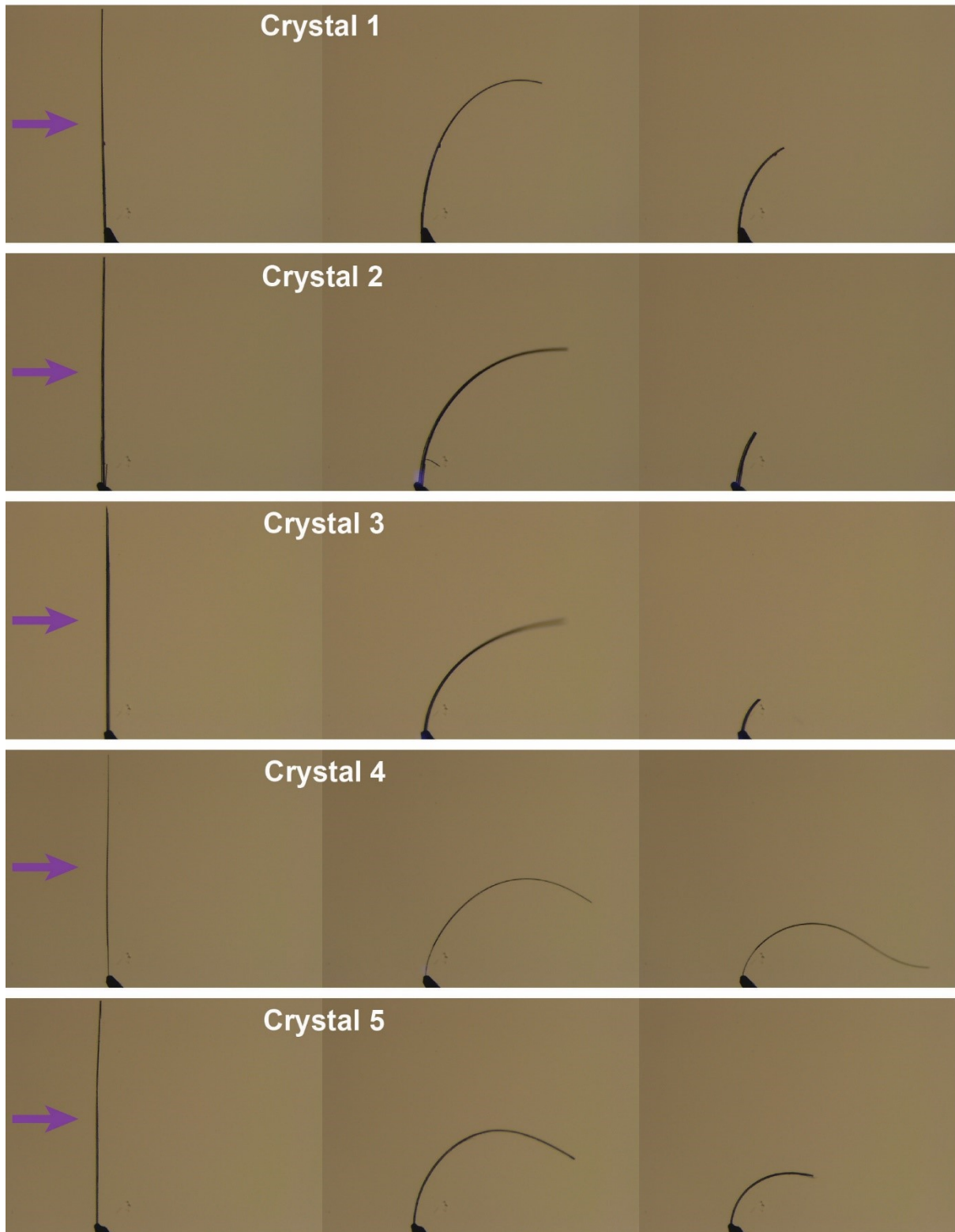
UV light power density (29.1 mW cm^{-2})



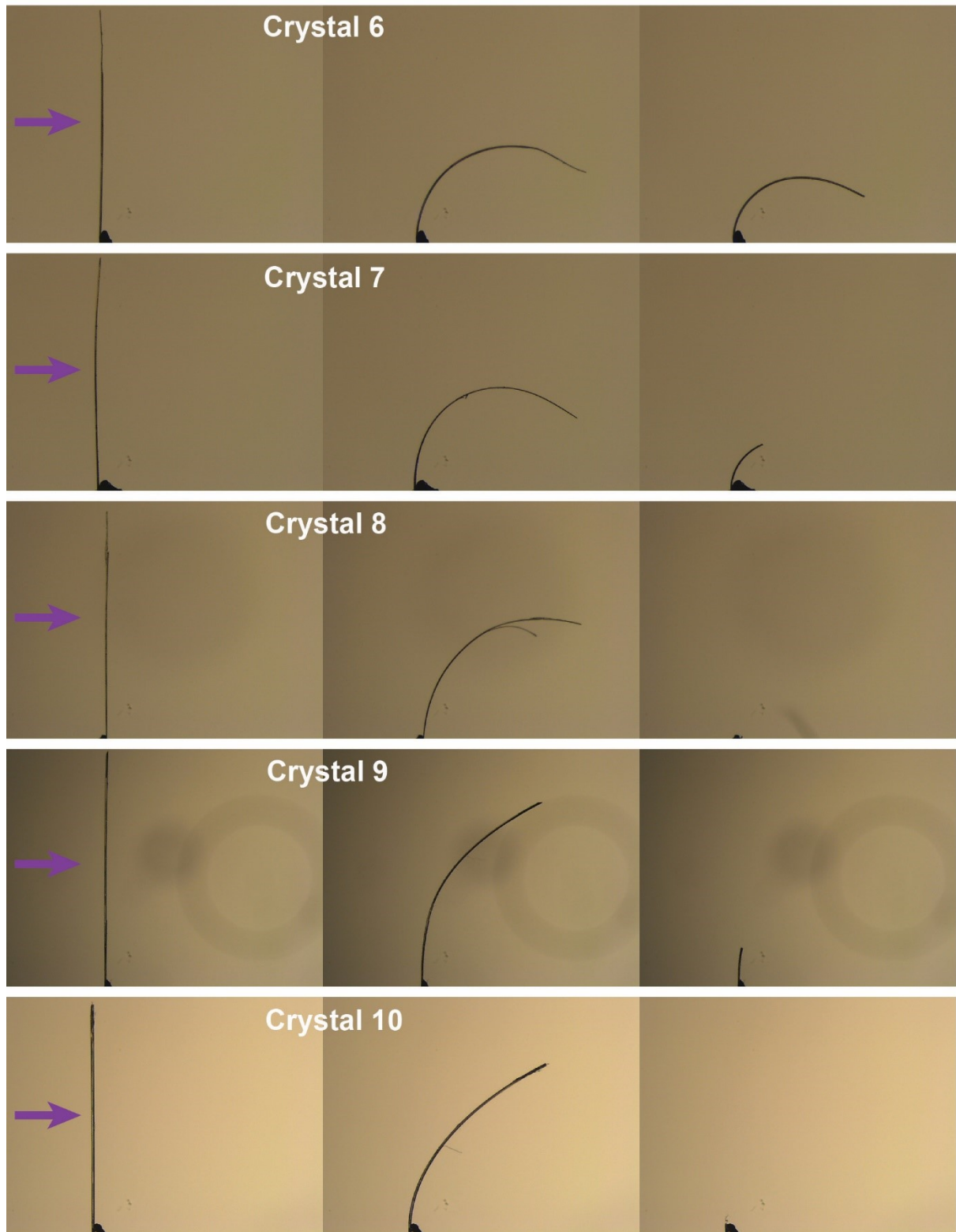
UV light power density (29.1 mW cm^{-2})



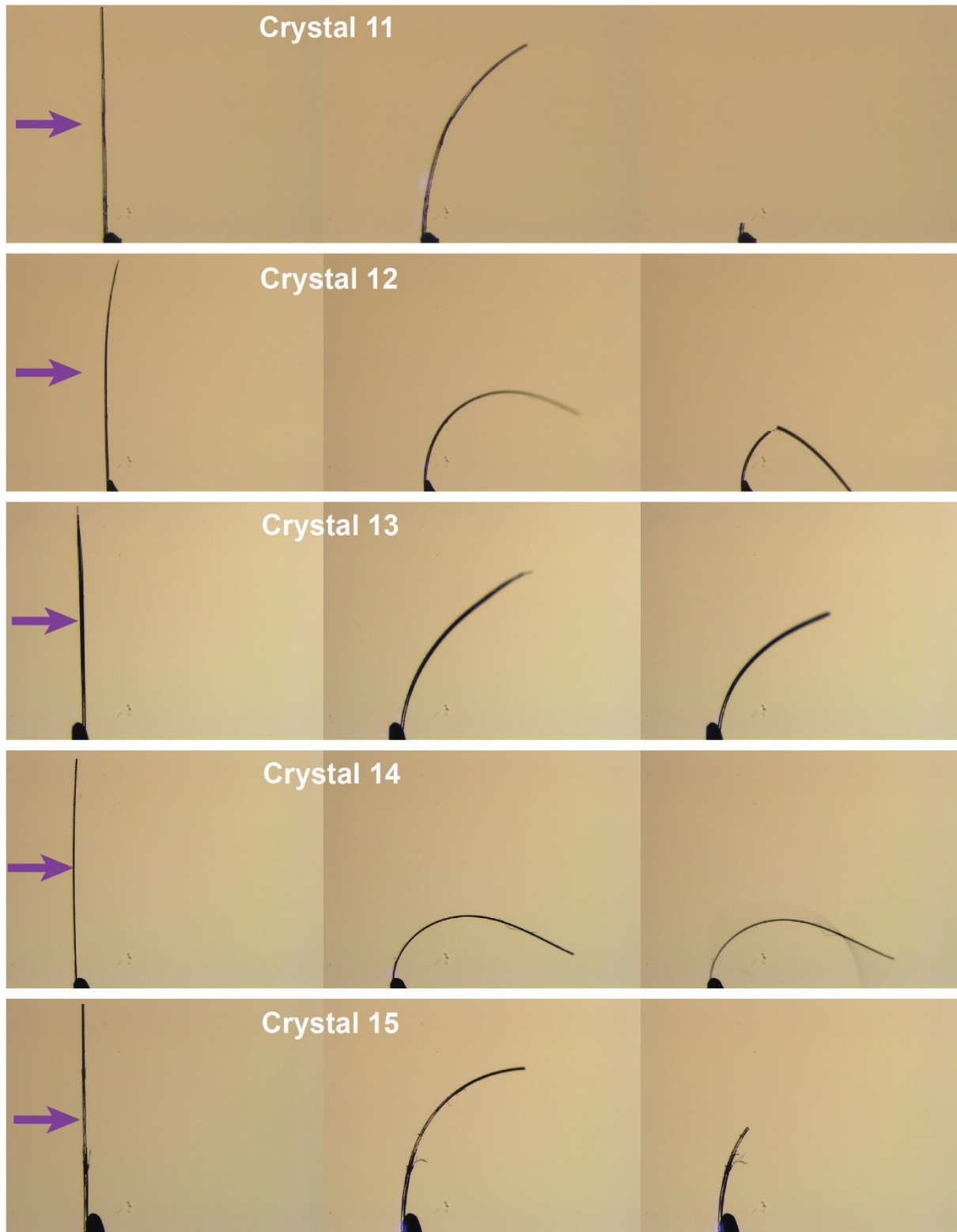
UV light power density (66.2 mW cm^{-2})



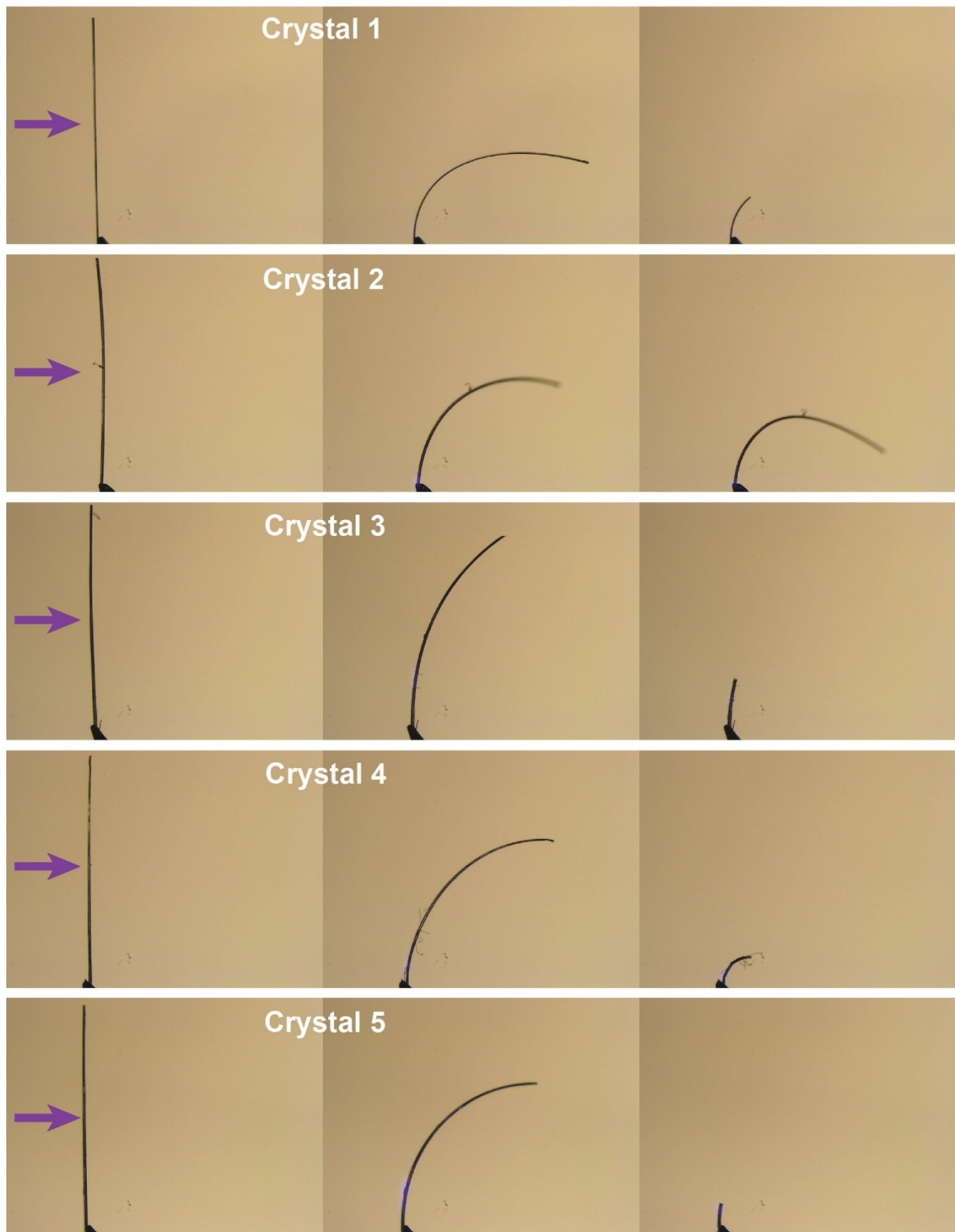
UV light power density (66.2 mW cm^{-2})



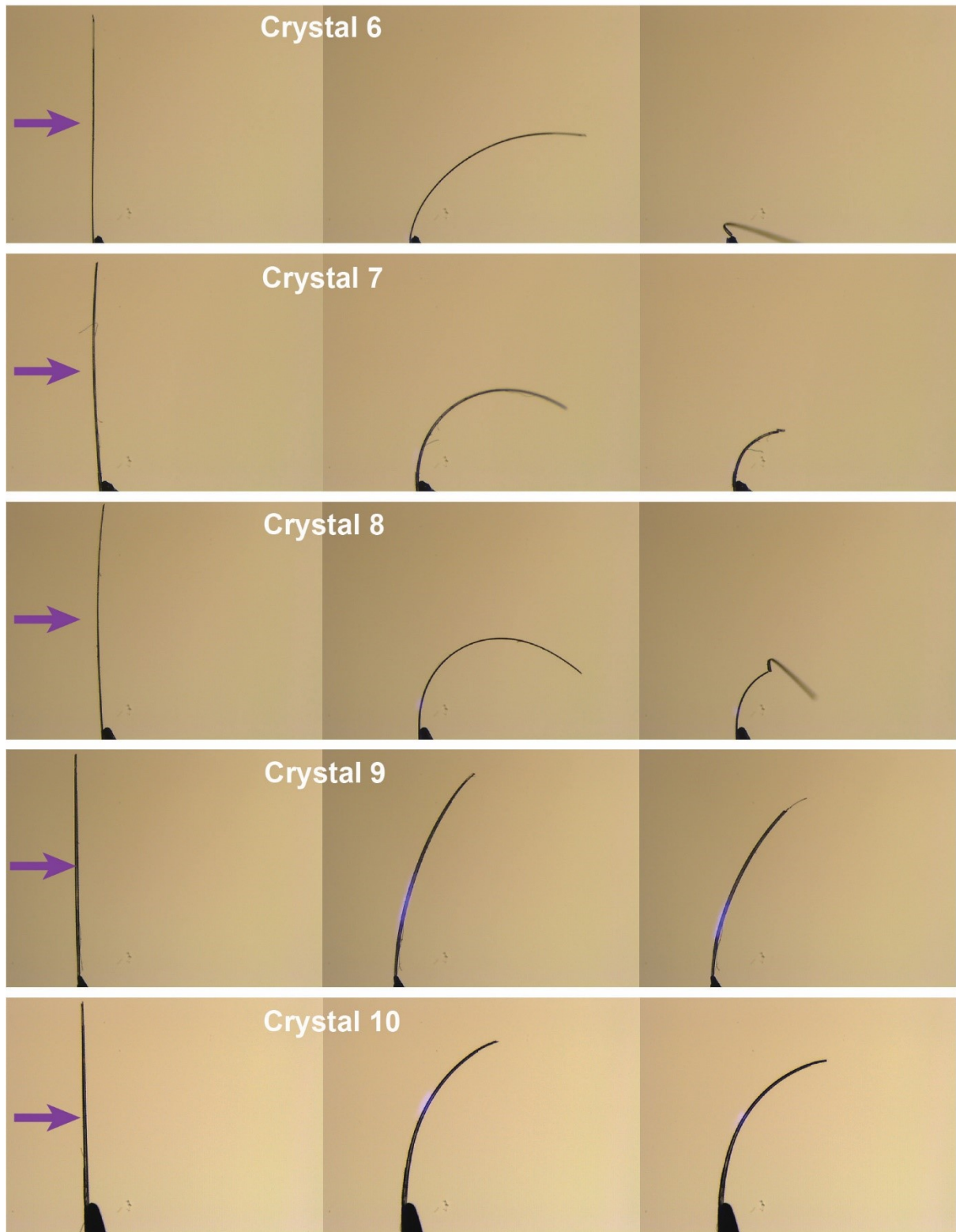
UV light power density (66.2 mW cm^{-2})



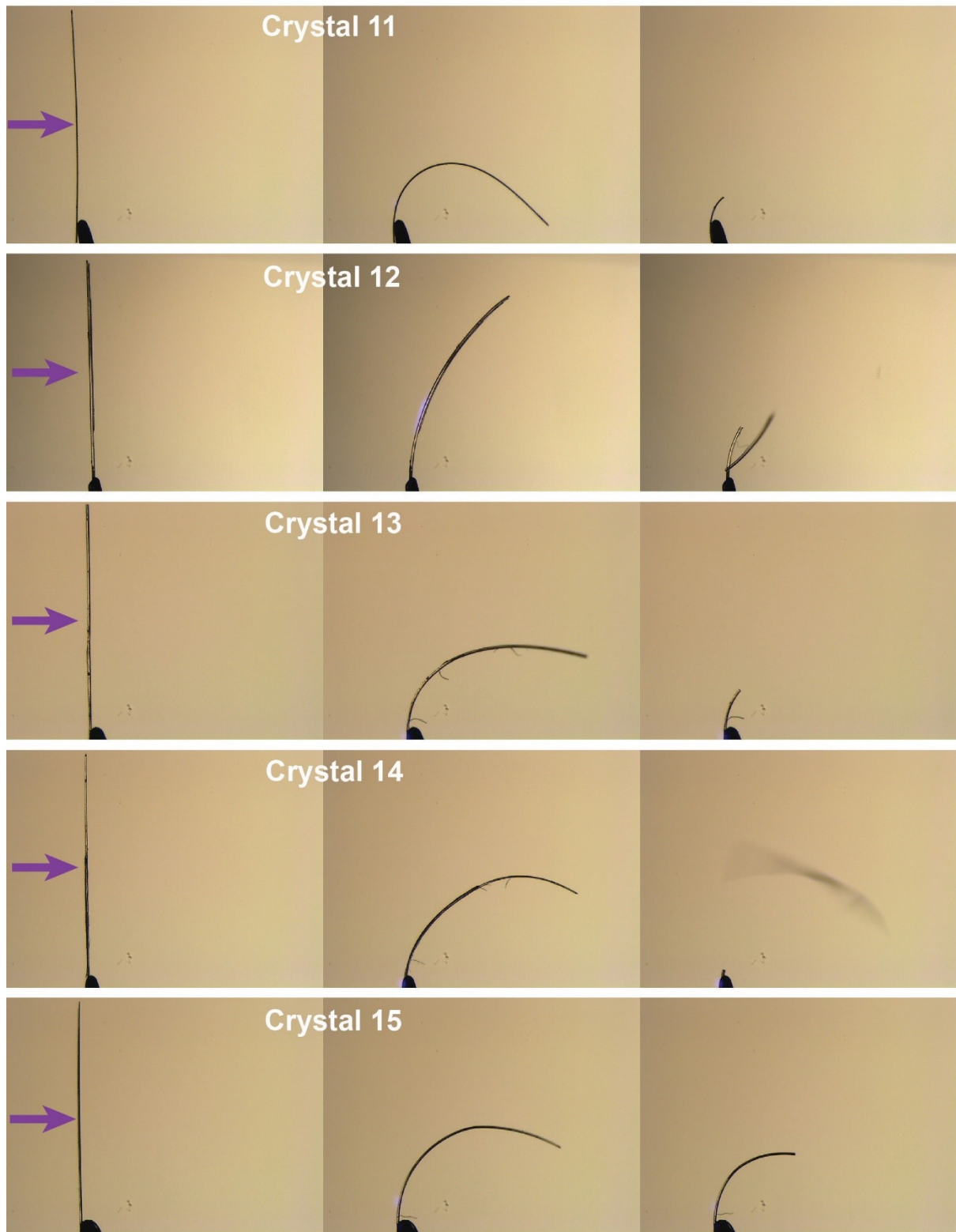
UV light power density (97.9 mW cm^{-2})



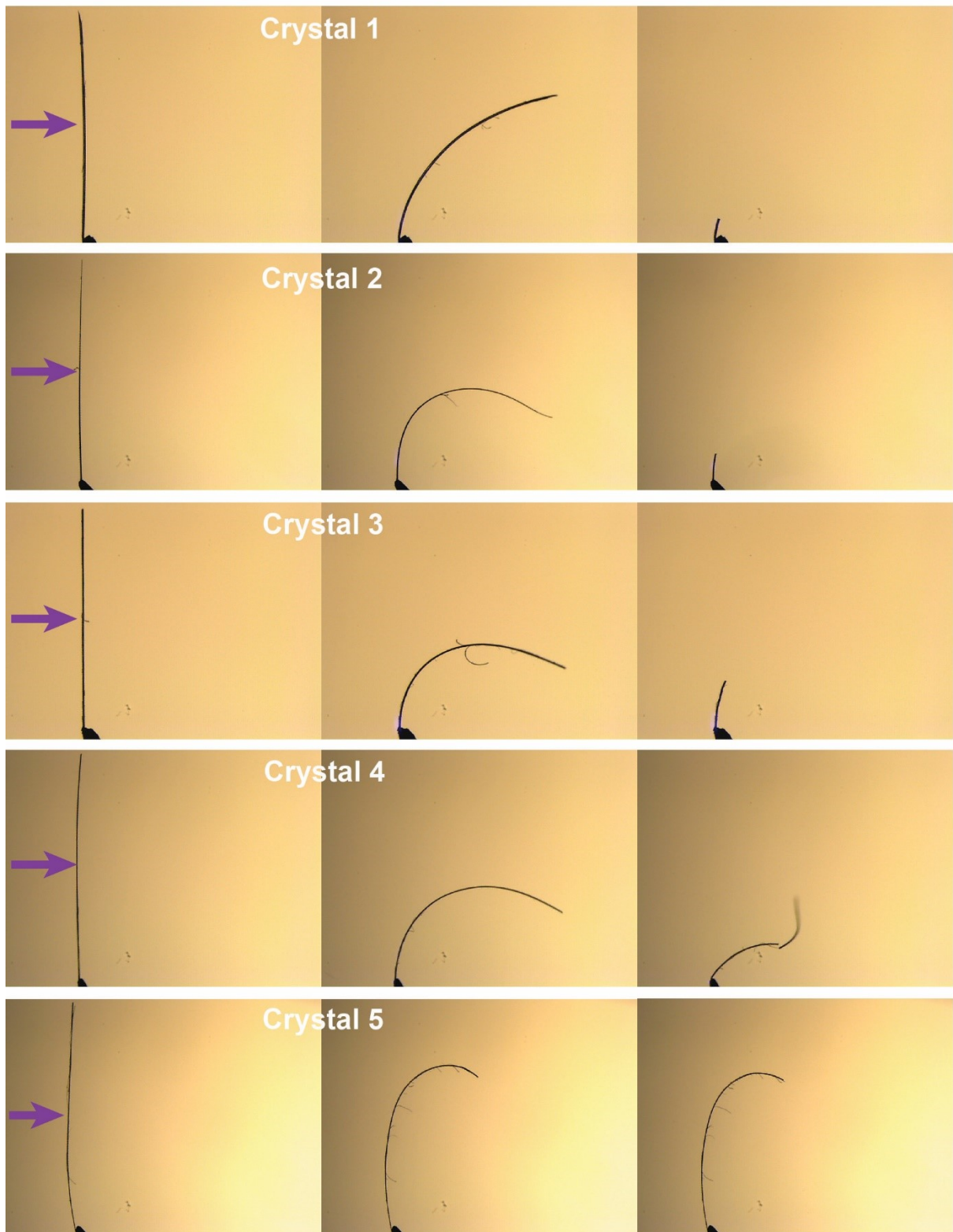
UV light power density (97.9 mW cm^{-2})



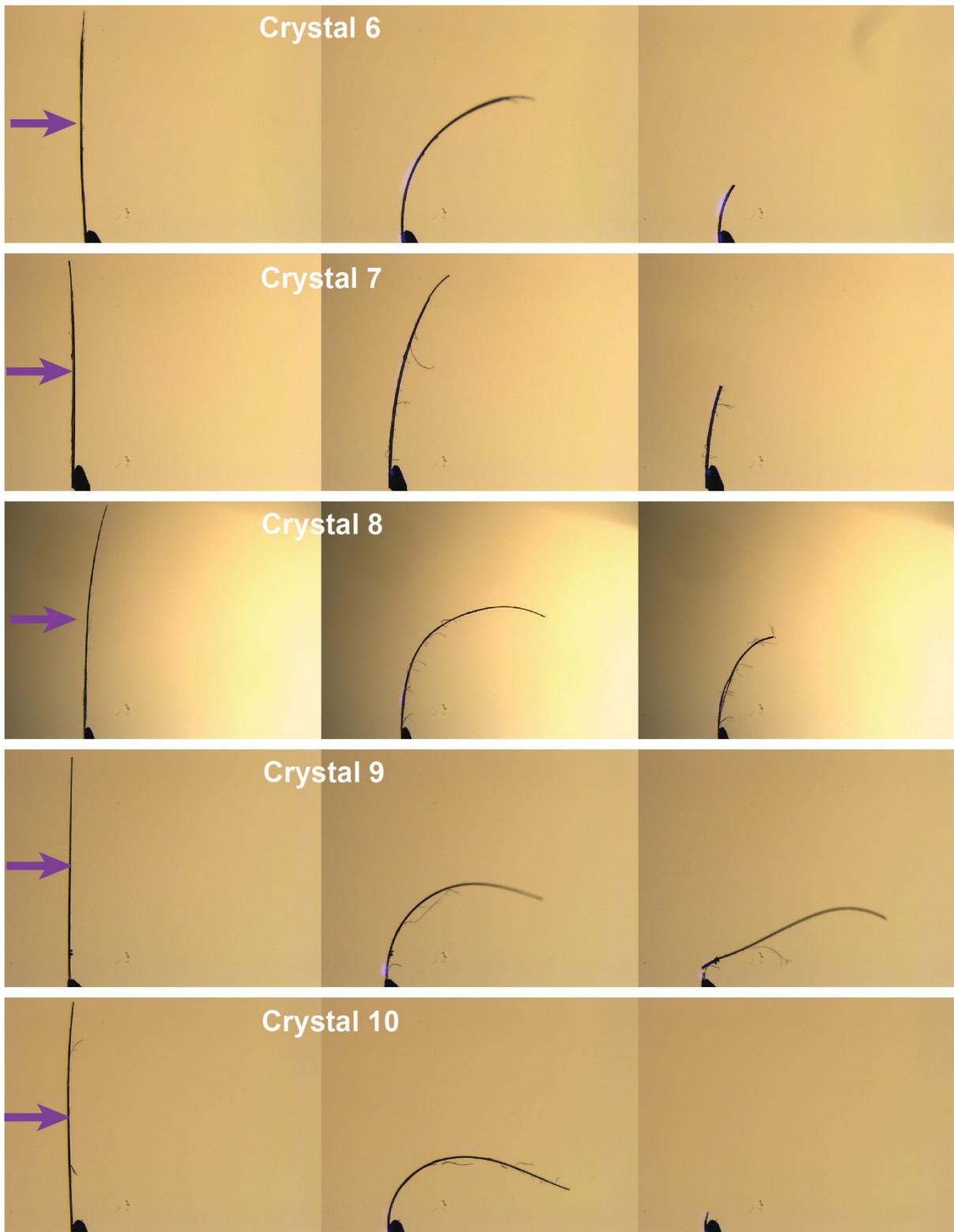
UV light power density (97.9 mW cm^{-2})



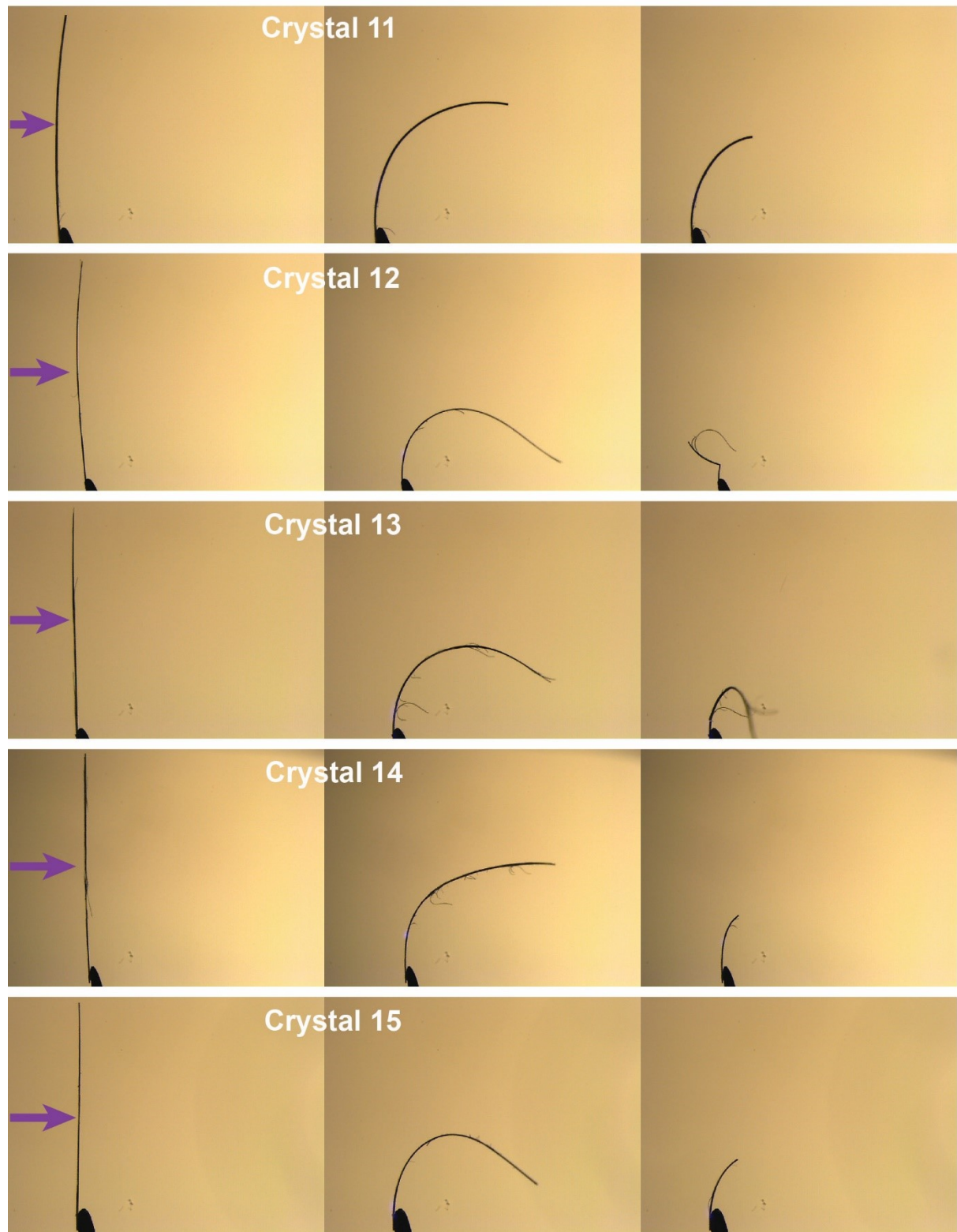
UV light power density (136.2 mW cm^{-2})



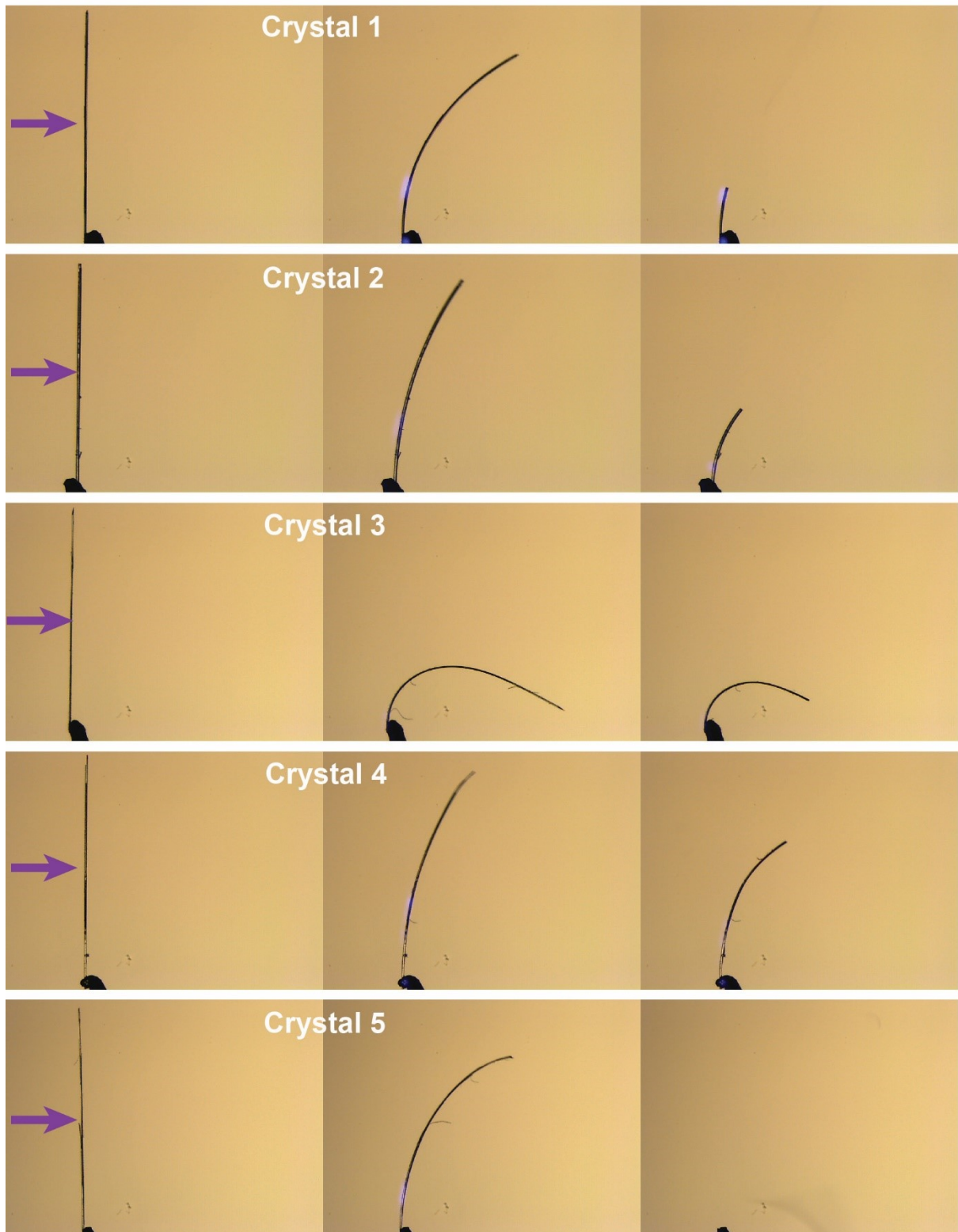
UV light power density (136.2 mW cm^{-2})



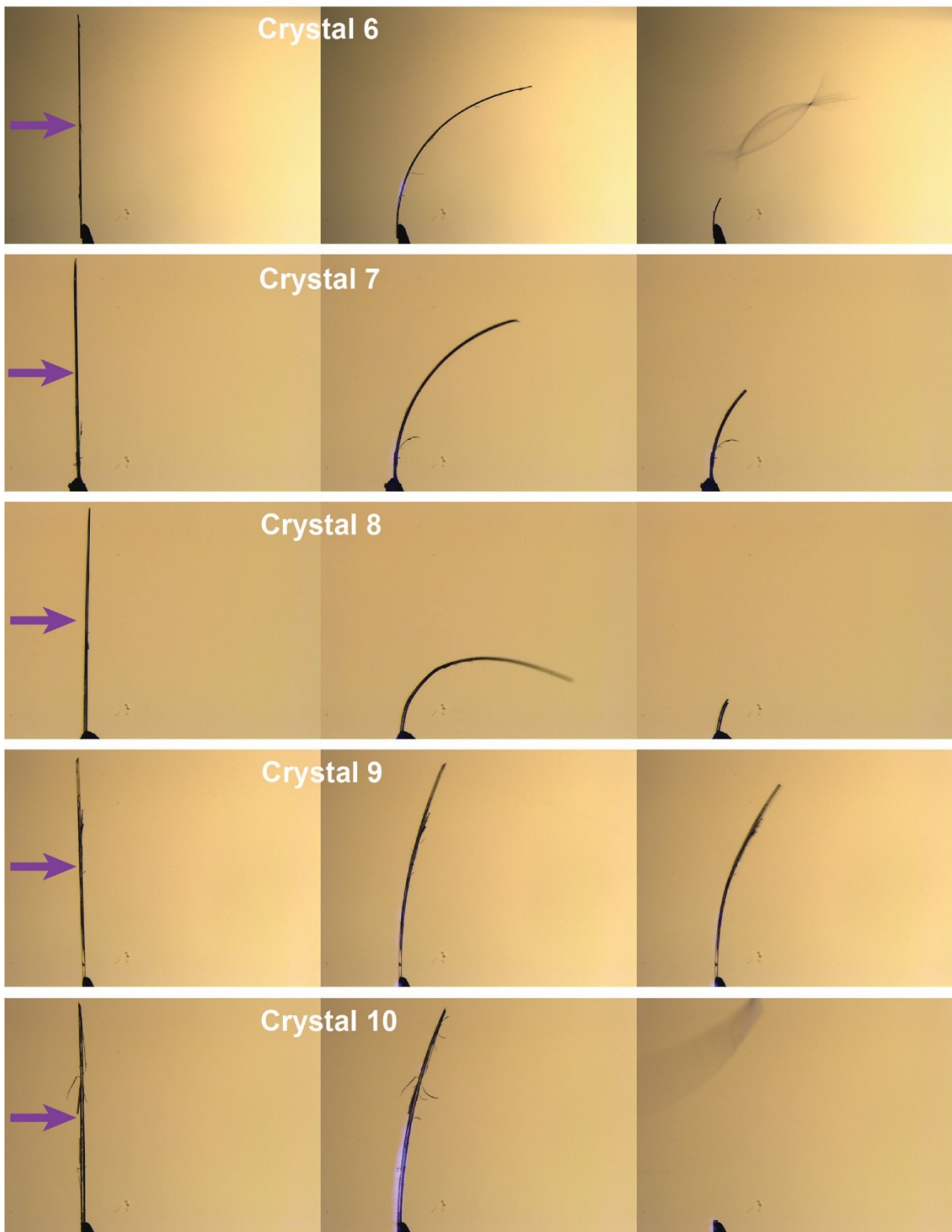
UV light power density (136.2 mW cm^{-2})



UV light power density (169.9 mW cm^{-2})



UV light power density (169.9 mW cm^{-2})



UV light power density (169.9 mW cm^{-2})

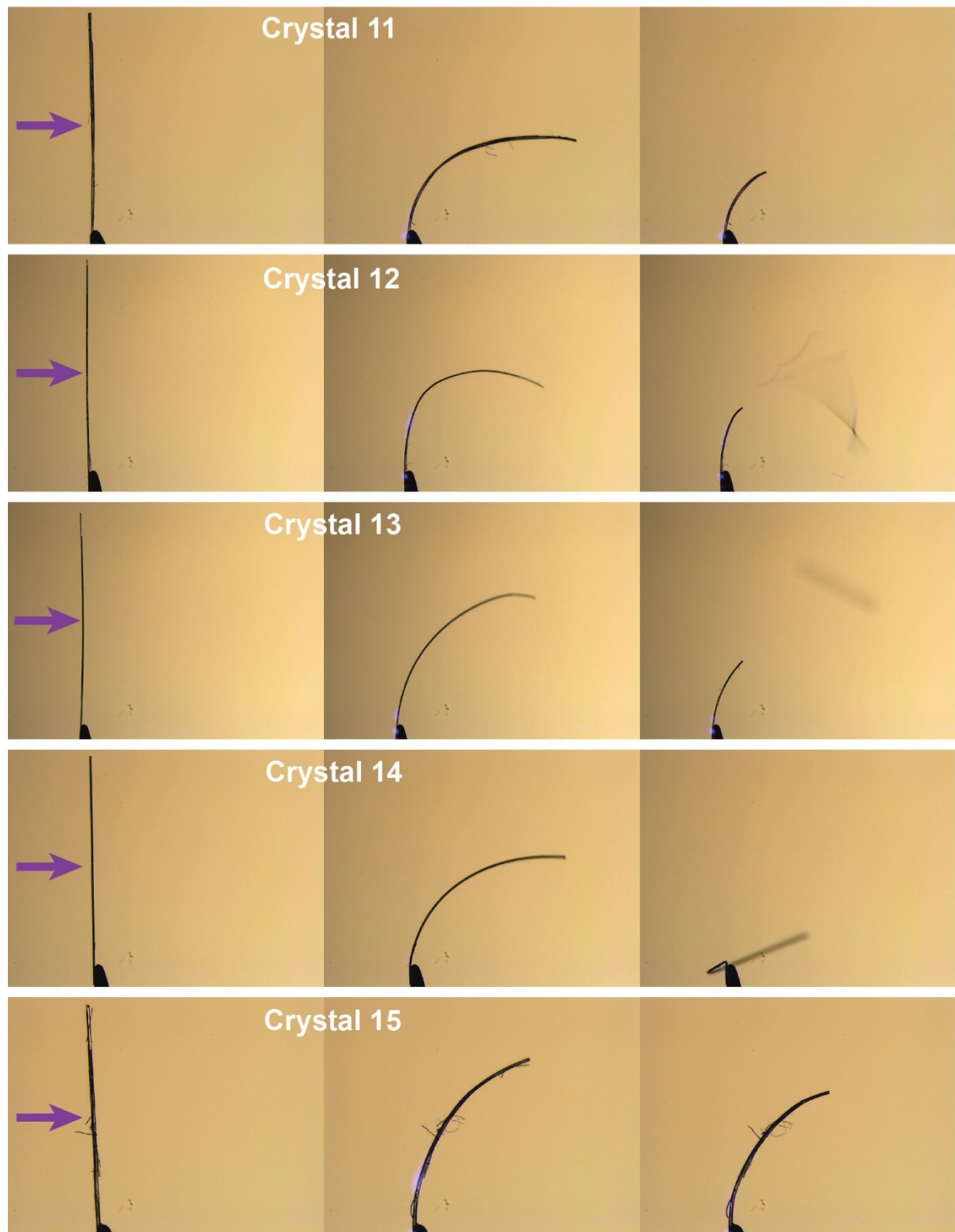


Figure S13. Photomechanical behaviour of **Ach** crystals in different UV light power density. Violet colour arrows signify the direction of UV light

3. Supporting tables.

Table S1. Basic crystallographic parameters of Ach

	Ach
Temperature / K	296.15
Radiation Source	Mo
Formula weight	273.317
Crystal system	Monoclinic
Space group	$P2_1/c$
a / Å	5.0509(5)
b / Å	12.3970(14)
c / Å	22.448(2)
α / °	90
β / °	93.489(8)
γ / °	90
Volume / Å ³	1403.0(3)
Z	4
Density / (g cm ⁻³)	1.294
μ / mm ⁻¹	0.082
sF_{000}	572.347
h_{\min}, h_{\max}	-6, 6
k_{\min}, k_{\max}	-14, 14
l_{\min}, l_{\max}	-26, 26
No. of measured reflections	12218
No. of unique reflections	2498
No. of reflections used	1426
$R_{\text{all}}, R_{\text{obs}}$	0.1341, 0.0688
$wR_{2,\text{all}}, wR_{2,\text{obs}}$	0.1887, 0.1535
$\Delta\rho_{\min,\max}$ / (e Å ⁻³)	-0.3758, 0.3830
$GooF$	1.0255
CCDC No.	2322612

Table S2. Summary of TD-DFT calculations for Ach (*E*) and Ach (*Z*)

Compound	Absorptions (nm)	Energy (eV)	Oscillator strength (f)	Transitions	Composition index (%)
Ach (<i>E</i>)	348.99	3.5526	0.5907	H→L	97.67
	247.11	5.0174	0.1481	H-6→L H-5→L H-2→L H-2→L+1 H-1→L H-1→L+1 H→L+3 H→L+4	21.33 3.65 3.43 5.87 12.17 12.73 6.54 23.91
Ach (<i>Z</i>)	321.56	3.8557	0.2709	H→L	95.77
	235.66	5.2611	0.1302	H-5→H+3 H-4→H H-4→H+1 H-2→H+1 H-2→H+3 H→H+3 H→H+4	3.83 2.69 20.65 4.66 2.34 31.68 23.48

Table S3. Mathematical equations used to calculate the various quantifiable parameters. For simplification, the radius (length of the crystal) is assumed to stay constant throughout the deflection. The equation $D = \theta R$ is a rational approximation for small angles of photomechanical bending.

Quantifiable parameter	Mathematical formulae
Calculation of elastic strain	$\varepsilon (\%) = t/2R \times 100$, where, ‘t’ and ‘R’ stand for the thickness and radius of curvature of the bent crystal respectively.
Tip displacement/ Tip deflection (<i>D</i>)	$D (\text{mm}) = [(x_2 - x_1)^2 + (y_2 - y_1)^2]^{1/2}$, where x_1, x_2 are the <i>x</i> coordinates and y_1, y_2 are the <i>y</i> coordinates of any two consecutive points on the trajectories of the crystal’s tip.
Angle of deflection (θ)	$\theta (\text{rad}) = (\text{Tip displacement}, D \text{ in mm}) / (\text{Length of the crystal}, R \text{ in mm rad}^{-1})$ $\text{Also, } \theta (\text{°}) = (180/\pi) \times \theta (\text{rad})$

Table S4. Dimensions of 75 crystals of Ach and their corresponding time to display photosalient effect when exposed to varied UV light power densities.

UV light power density (29.1 mW cm⁻²)

Crystal No.	Length (mm)	Width (mm)	Thickness (mm)	Surface Area (mm ²)	Time (Sec)
1	4.59	0.04	0.02	0.1836	2.89
2	4.85	0.06	0.04	0.291	13.49
3	4.14	0.05	0.035	0.207	7.33
4	5.63	0.04	0.02	0.2252	6.91
5	4.09	0.07	0.03	0.2863	4.92
6	4.8	0.04	0.03	0.192	8.26
7	4.77	0.03	0.03	0.1431	6.75
8	3.93	0.04	0.02	0.1572	28.97
9	4.04	0.06	0.04	0.2424	8.10
10	4.2	0.05	0.04	0.21	4.93
11	3.63	0.05	0.04	0.1815	4.19
12	4.32	0.05	0.035	0.216	3.71
13	5.33	0.04	0.03	0.2132	14.91
14	5.34	0.12	0.05	0.6408	12.15
15	4.93	0.08	0.05	0.3944	31.48

UV light power density (66.2 mW cm⁻²)

Crystal No.	Length (mm)	Width (mm)	Thickness (mm)	Surface Area (mm ²)	Time (Sec)
1	4	0.05	0.04	0.2	5.46
2	3.78	0.065	0.06	0.2457	18.17
3	4.02	0.08	0.03	0.3216	4.25
4	4.79	0.03	0.02	0.1437	2.13
5	4.8	0.04	0.03	0.192	10.51
6	4.69	0.04	0.03	0.1876	9.86
7	5.42	0.09	0.045	0.4878	10.28
8	6.74	0.06	0.04	0.4044	6.26
9	10.21	0.14	0.12	1.4294	18.17
10	6.49	0.11	0.06	0.7139	15.48
11	2.78	0.05	0.05	0.139	2.22
12	4.75	0.08	0.04	0.38	4.08
13	4.79	0.07	0.04	0.3353	10.57
14	4.33	0.06	0.04	0.2598	12.10
15	3.99	0.05	0.04	0.1995	9.06

UV light power density (97.9 mW cm^{-2})

Crystal No.	Length (mm)	Width (mm)	Thickness (mm)	Surface Area (mm ²)	Time (Sec)
1	5.84	0.07	0.05	0.4088	4.23
2	4.82	0.07	0.04	0.3374	8.39
3	5.55	0.09	0.08	0.4995	3.09
4	5.01	0.06	0.06	0.3006	2.80
5	5.32	0.08	0.06	0.4256	4.09
6	5.48	0.07	0.04	0.3836	1.66
7	4.52	0.09	0.05	0.4068	6.92
8	5.77	0.09	0.04	0.5193	4.16
9	6.55	0.11	0.07	0.7205	2.10
10	4.44	0.07	0.05	0.3108	4.30
11	5.73	0.065	0.04	0.37245	7.89
12	7.62	0.12	0.08	0.9144	3.30
13	4.34	0.05	0.045	0.217	16.54
14	5.05	0.07	0.06	0.3535	6.20
15	4.81	0.06	0.05	0.2886	5.37

UV light power density (136.2 mW cm^{-2})

Crystal No.	Length (mm)	Width (mm)	Thickness (mm)	Surface Area (mm ²)	Time (Sec)
1	5.33	0.06	0.05	0.3198	2.22
2	7.81	0.09	0.05	0.7029	1.80
3	5.9	0.05	0.04	0.295	3.01
4	7.52	0.05	0.04	0.376	1.47
5	8.89	0.06	0.04	0.5334	6.08
6	4.56	0.06	0.04	0.2736	2.36
7	5.5	0.09	0.08	0.495	1.33
8	9.63	0.11	0.07	1.0593	4.13
9	4.88	0.06	0.04	0.2928	3.91
10	3.88	0.05	0.03	0.194	4.78
11	6.13	0.06	0.06	0.3678	3.10
12	7.1	0.08	0.04	0.568	1.12
13	6	0.07	0.05	0.42	2.28
14	8.05	0.09	0.05	0.7245	2.92
15	5.62	0.06	0.04	0.3372	2.78

UV light power density (169.9 mW cm^{-2})

Crystal No.	Length (mm)	Width (mm)	Thickness (mm)	Surface Area (mm ²)	Time (Sec)
1	5.18	0.07	0.06	0.3626	1.17
2	4.22	0.06	0.05	0.2532	1.11
3	5.08	0.05	0.05	0.254	22.18
4	5.16	0.06	0.05	0.3096	0.49
5	5.51	0.065	0.05	0.35815	1.01
6	8.04	0.07	0.06	0.5628	1.94
7	4.8	0.08	0.05	0.384	1.34
8	3.78	0.06	0.04	0.2268	5.29
9	6.03	0.09	0.06	0.5427	0.62
10	5.7	0.11	0.07	0.627	1.01
11	5.16	0.08	0.07	0.4128	3.33
12	7	0.07	0.05	0.49	1.35
13	7.08	0.05	0.05	0.354	0.84
14	5.51	0.05	0.04	0.2755	1.73
15	4.56	0.07	0.06	0.3192	5.81

4. Optimized coordinates.

Optimized coordinates of Ach (E) at B3LYP/6-31G(d) level

0 1

O 2.69368652 -2.14424757 -0.13945972
 N 1.54606848 -0.16793741 0.06581140
 N 0.32419204 -0.75479218 0.07658983
 C 3.97491361 -0.13000901 0.00994383
 C 2.70462097 -0.93143554 -0.02550051
 C -3.21179294 0.35228016 -0.03698288
 C -2.06548786 -0.51254075 0.06947925
 C -0.70013335 0.02190956 0.03450595
 H -0.56544579 1.10818844 -0.02076132
 C -4.52185085 -0.23743746 0.01911412
 C 4.09247386 1.11596859 0.64369465
 H 3.24683891 1.54777015 1.17288980
 C -2.25348918 -1.88226575 0.21396305

H	-1.37689654	-2.51674663	0.29153788
C	5.10281883	-0.69665872	-0.59969975
H	5.00236426	-1.67295620	-1.06244416
C	-3.13198635	1.76413673	-0.19962171
H	-2.16524284	2.25230017	-0.25691269
C	-4.65472815	-1.64119462	0.17004907
H	-5.65320971	-2.06978065	0.21027834
C	-3.54074253	-2.44629675	0.26275941
H	-3.64851125	-3.52126083	0.37712618
C	5.31306552	1.79176870	0.64774418
H	5.39676528	2.75095141	1.15128997
C	-5.66922727	0.59605207	-0.08048592
H	-6.65082619	0.13026608	-0.03471322
C	-4.26417258	2.54293815	-0.29409925
H	-4.16821313	3.61825679	-0.41827302
C	6.42533757	1.23025479	0.01871327
H	7.37505278	1.75833094	0.02055125
C	-5.54974942	1.95683589	-0.23293097
H	-6.43506502	2.58203128	-0.30826716
C	6.31811880	-0.01718772	-0.60221432
H	7.18440048	-0.46104344	-1.08505163
H	1.60874082	0.84407022	-0.02896981

Absolute Energy = -879.061435 a.u.

Number of imaginary frequencies = 0

Optimized coordinates of Ach (Z) at B3LYP/6-31G(d) level

0 1			
O	2.97536754	2.51992845	0.15728993
N	1.12883023	1.15734405	0.21929082
N	0.24876106	2.18298048	0.36121094
C	3.31188466	0.18497695	-0.22641858
C	2.48514247	1.40970865	0.05340909
C	-2.82245897	0.25382415	0.02072056

C	-1.64263693	0.58989437	0.76754556
C	-0.99142605	1.91088830	0.57241015
H	-1.63019427	2.79213064	0.61779571
C	-3.48731869	-0.98761664	0.29254465
C	2.80992688	-0.97651375	-0.83220299
H	1.77426935	-1.02837582	-1.15802769
C	-1.16746549	-0.29661695	1.72329223
H	-0.29877725	-0.02625747	2.31810547
C	4.66996626	0.24454352	0.11609154
H	5.04817508	1.15949267	0.56017844
C	-3.35406735	1.09842269	-0.99153653
H	-2.84441450	2.02645746	-1.23088885
C	-2.95777452	-1.85972704	1.28111015
H	-3.46951078	-2.79855589	1.47843055
C	-1.82132085	-1.52368407	1.97881264
H	-1.42601967	-2.19038381	2.73992347
C	3.64909648	-2.06541309	-1.07100580
H	3.25250577	-2.95626360	-1.55031120
C	-4.65855772	-1.31987388	-0.43959673
H	-5.15613127	-2.26267770	-0.22508628
C	-4.49280620	0.74663255	-1.68262004
H	-4.88311588	1.40651532	-2.45247165
C	4.99497478	-2.00497623	-0.70663617
H	5.64686344	-2.85467707	-0.89106795
C	-5.15502739	-0.47196505	-1.40309438
H	-6.05185560	-0.73782999	-1.95574945
C	5.50443327	-0.84566939	-0.11534480
H	6.55371497	-0.79171898	0.16177901
H	0.79102340	0.19943424	0.24067542

Absolute Energy = -879.057079 a.u.

Number of imaginary frequencies = 0

5. References

- S1 P. Gupta, T. Panda, S. Allu, S. Borah, A. Baishya, A. Gunnam, A. Nangia, P. Naumov and N. K. Nath, *Cryst. Growth Des.*, 2019, **19**, 3039–3044.
- S2 Bruker, *APEX II*, Bruker AXS Inc., Madison, Wisconsin, USA, 2012.
- S3 Bruker, *SAINT*, Bruker AXS Inc., Madison, Wisconsin, USA, 2012.
- S4 Bruker, *SADABS*, Bruker AXS Inc., Madison, Wisconsin, USA, 2001.
- S5 G. M. Sheldrick, *Acta Crystallogr., Sect. A: Found. Adv.* 2015, **71**, 3–8.
- S6 G. M. Sheldrick, *Acta Crystallogr., Sect. A: Found. Adv.* 2008, **64**, 112–122.
- S7 C. B. Hübschle, G. M. Sheldrick, B. Dittrich, *J. Appl. Crystallogr.* 2011, **44**, 1281– 1284.
- S8 O. V. Dolomanov, L. J. Bourhis, R. J. Gildea, J. A. K. Howard, H. Puschmann, *Journal of applied crystallography*, 2009, **42**(2), 339-341.
- S9 M. J. Frisch et al. Gaussian 09, Revision E.01, Gaussian, Inc., Wallingford CT, 2013.
- S10 W. Kohn, A. D. Becke, R. G. Parr, *J. Phys. Chem.* 1996, **100**, 12974–12980.
- S11 R. Ditchfield, W. J. Hehre, J. A. Pople, *J. Chem. Phys.* 1971, **54**, 724.
- S12 M. S. Gordon, *Chem. Phys. Lett.* 1980, **76**, 163-68.

6. Legends to the Supporting Movies:

Video S1: Elastic bending of **Ach** single crystal.

Video S2: Photoresponsive behaviour of a bunch of **Ach** single crystals.

Video S3: Photoresponsive behaviour of individual **Ach** single crystals.